

## Experimental Study of the Relative Phase between $J/\psi$ Production Amplitudes

---

**M. Destefanis**<sup>\*†</sup>

*Università degli Studi di Torino and INFN*

*E-mail:* [marco.destefanis@to.infn.it](mailto:marco.destefanis@to.infn.it)

QCD is undoubtedly a well established theory that is able to describe strong interactions. Yet several open issues could be investigated by means of modern existing and forthcoming facilities, that would provide more tests of this theoretical framework. In particular a more detailed investigation in the kinematic region in the vicinity of  $J/\psi$  production can probe the validity of the QCD perturbative approach. In this energy range an interference between the resonant  $e^+e^- \rightarrow J/\psi \rightarrow hadrons$  and the non-resonant  $e^+e^- \rightarrow hadrons$  amplitudes can, in principle, occur. In a perturbative approach those amplitudes are expected to be all almost real, i.e. the relative phase between the above cited amplitudes is expected to be compatible with either  $0^\circ$  or  $180^\circ$ , implying a maximal interference scenario. Nevertheless, data available in the literature appear to suggest a no interference scenario implying a relative phase of  $\sim 90^\circ$ . An experimental approach able to provide a measurement of the relative phase in a model independent way, and in particular its deployment and its latest results in the BESIII scenario, will be discussed in details.

*International Winter Meeting on Nuclear Physics,  
21-25 January 2013  
Bormio, Italy*

---

<sup>\*</sup>Speaker.

<sup>†</sup>For the BESIII Collaboration.

## 1. Introduction

The validity of the QCD perturbative approach and its limits can be investigated in the energy region around the  $J/\psi$  resonance by studying the interaction between the strong and the electromagnetic decay amplitudes.

The existence of an interference between the resonant  $e^+e^- \rightarrow J/\psi \rightarrow leptons$  and non-resonant  $e^+e^- \rightarrow leptons$  has already been observed at SPEAR (SLAC)[1] and at BESII (IHEP)[2] by investigating the muon pair final state. An interference in the hadronic final states could be probed as well by an energy scan around the  $J/\psi$  resonance peak. The  $\simeq 93$  KeV  $J/\psi$  decay width could be interpreted as a proof that the perturbative regime holds in this energy region. In the PQCD approach, the strong  $A_{3g}$  (Fig. 1a) and the electromagnetic  $A_\gamma$  (Fig. 1b)  $J/\psi$  resonant amplitudes are predicted to be almost real [3]. The non-resonant electromagnetic amplitude  $A_{EM}$  (Fig. 1c) is expected to be almost real as well. If those assumptions are correct, maximal inter-

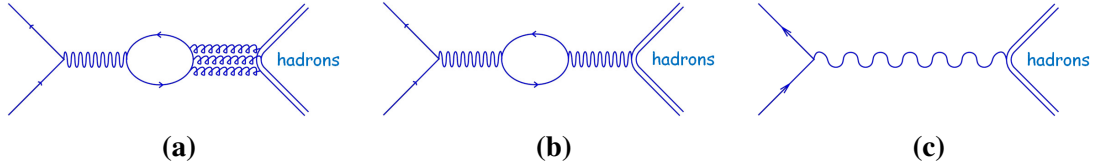


**Figure 1:** Diagram for the process  $e^+e^- \rightarrow hadrons$ : (a) strong  $A_{3g}$ , (b) electromagnetic  $A_\gamma$ , and (c) non resonant  $A_{EM}$  contributions.

ference between the above mentioned amplitudes should occur, corresponding to a relative phase of  $\sim 0^\circ/180^\circ$ . In contrast, the experimental data suggest an unexpected relative phase around  $90^\circ$ . Indeed, no-interference patterns [3, 4, 5, 6, 7, 8] were found in a variety of investigated  $J/\psi$  decays into  $N\bar{N}$ ,  $VP$ ,  $PP$ , and  $VV$ , where  $N$  stand for nucleon, and  $V$  and  $P$  for vector and pseudoscalar mesons respectively. A model independent way to investigate the relative phase between the strong and the electromagnetic amplitudes is to search for interference at different  $Q^2$  values.

In both SPEAR[1] and BESII[2] experiments, an inclusive set of final state measurements provided no indication of an interference, but, as soon as exclusive final states were considered, dips in the cross sections, characteristics of interference, could be detected. An inclusive set of different exclusive measurements is the only feasible approach, since, in inclusive measurements, interference patterns are expected to vanish.

In order to explore the different experimental scenarios, we focused our investigations on the  $e^+e^- \rightarrow p\bar{p}$ ,  $e^+e^- \rightarrow \rho\pi$ , and  $e^+e^- \rightarrow 5\pi$  interactions. We selected these final states because they have already been widely investigated, they are characterised by a significantly different cross section in the energy region around the 3 GeV range far from the  $J/\psi$  peak (the so called non-resonant “continuum” region), and they have quite different branching fractions. Different final states will be investigated as well at a later time.

The excellent performance of the BEijing Spectrometer III (BESIII) [9], hosted on the BEPCII  $e^+e^-$  collider at the Institute of High Energy Physics (IHEP) in Beijing, offers the appropriate scenario for our measurements. The BEPCII (Beijing Electron-Positron Collider II) is designed to provide an instant Luminosity up to  $10^{33} \text{ cm}^{-2} \text{ s}^{-1}$  with beam currents up to 0.93 A. The beam energy (up to 2.3 GeV) can be tuned according to the required center of mass energy, for example

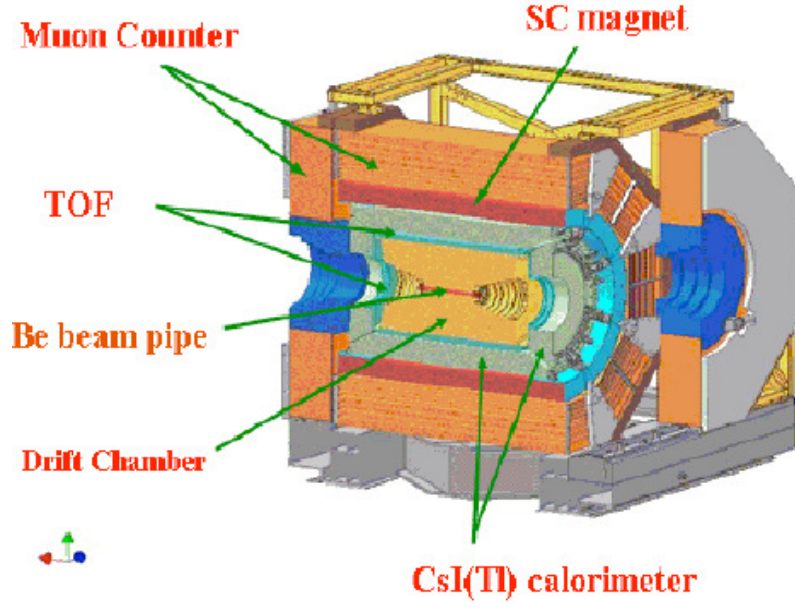


Figure 2: 3D view of the BESIII spectrometer.

to produce different charmonium resonances as  $J/\psi$ ,  $\psi'$  or  $\psi''$ . The BESIII spectrometer, shown in Fig.2, is characterized by a shell like structure, which provides a wide geometrical acceptance, 93% of  $4\pi$ . At increasing distances from the interaction point, it hosts a 43-layer small-celled, helium-based main drift chamber (MDC) chamber, a time-of-flight system (TOF) for particle identification, and an electromagnetic calorimeter (EMC) composed of 6240 CsI (Tl) crystals arranged in a cylindrical shape (barrel) plus two end-caps. The above-mentioned detectors operate inside a 1T solenoidal magnetic field. The magnet iron yoke is segmented to host a muon chamber system composed of resistive plate chambers (for a total of  $1000\text{ m}^2$ ) arranged in 9 layers in the barrel and 8 layers in the end-caps. An electromagnetic calorimeter which covers the zero degree region, ZDD (Zero Degree Detector), was installed on August 2011 for Initial State Radiations (ISR) studies.

The initial state radiation, crucial when considering  $e^+ e^-$  interactions, is taken into account in the procedure adopted for the investigation that is reported here. A simple model of the cross section

$$\sigma[nb] = 12\pi B_{in} B_{out} \left[ \frac{\hbar c}{W} \right]^2 \cdot 10^7 \cdot \left| \frac{C_1 + C_2 e^{i\phi}}{W - W_{res} + i\Gamma/2} + C_3 e^{i\phi} \right|^2 \quad (1.1)$$

was assumed for both the event generation and the fitting procedure. In eq. 1.1,  $B_{in}$  and  $B_{out}$  are the branching ratios of the  $J/\psi \rightarrow e^+ e^-$  and  $J/\psi \rightarrow final\ state$  respectively;  $W_{res}$  and  $\Gamma$  are the mass and width of the  $J/\psi$  resonance;  $W$  is the energy of the final state;  $C_1$  and  $C_2$  are the strong and the electromagnetic resonance amplitudes;  $C_3$  is the “continuum” electromagnetic amplitude. The energy carried by the ISR photons was limited to 300 MeV, a conservative assumption, since it accounts as almost 20% of the  $E_{CM}$ . The beam energy spread (0.92 MeV) was taken into account as well. Fig. 3 shows the expected cross section when no correction to the beam energy is accounted for. An extremely narrow  $J/\psi$  peak and a dip, in the  $0^\circ$  scenario, can be here observed. When beam spread effects are included, as shown in Fig. 4, one can start to identify a broadening of the

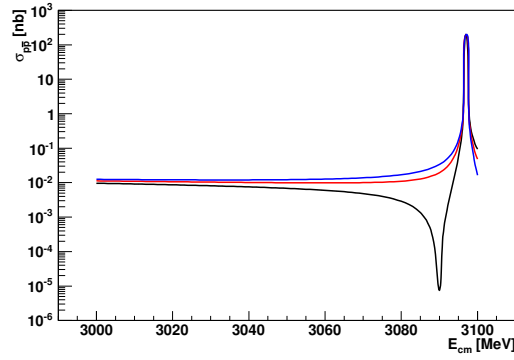


**Figure 3:** Uncorrected line-shapes for the maximum interference,  $0^\circ$  (black) and  $180^\circ$  (blue), and the no interference,  $90^\circ$  (red), scenarios.

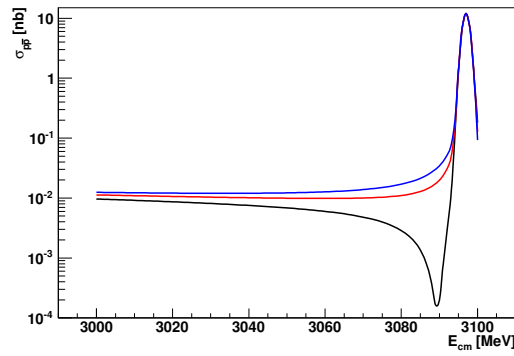


**Figure 4:** Line-shapes for the maximum interference,  $0^\circ$  (black) and  $180^\circ$  (blue), and the no interference,  $90^\circ$  (red), scenarios once beam spread has been accounted for.

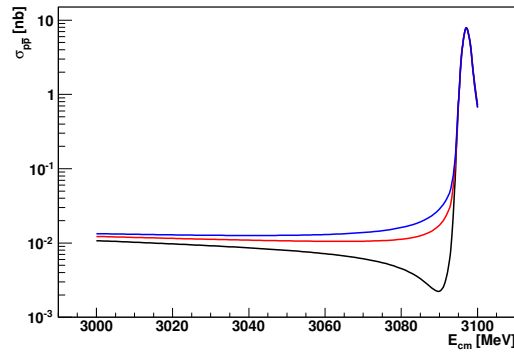


**Figure 5:** Line-shapes for the maximum interference,  $0^\circ$  (black) and  $180^\circ$  (blue), and the no interference,  $90^\circ$  (red), scenarios once beam spread and initial state radiation have been accounted for.

two above mentioned structures. Figure 5 shows the combined effects of the beam spread and of the initial state radiation to the cross section, which produces an evident broadening of the  $J/\psi$  peak and the interference minimum. Although the final optimization was performed in the case of

the process  $e^+e^- \rightarrow p\bar{p}$  only, the reconstruction of the relative phase was evaluated for all of the above mentioned final states.

The selection of the energy points is also critical, since we aim to obtain an inclusive set of exclusive measurements. To obtain an effective determination of the relative phase, an optimization was performed that takes into account that for the maximum interference scenario with a relative phase  $\Delta\varphi = 0^\circ$  and for the no interference scenario with a  $\Delta\varphi = 90^\circ$ .

For our measurements, two points at low energy values (low  $W$ ) are needed to anchor the cross section to the “continuum” and to its slope. To investigate the maximum interference scenario, two more energy points have been chosen in the expected region of the cross section dip for the  $e^+e^- \rightarrow p\bar{p}$  and  $e^+e^- \rightarrow \rho\pi$  processes. A fifth point has been chosen at the beginning of the Breit-Wigner, where the resonant amplitudes should start to dominate the  $e^+e^- \rightarrow p\bar{p}$  process. Since the literature suggests a no-interference scenario, the gradient of  $\Delta\varphi = 90^\circ$   $[(\sigma_{90} - \sigma_i)/\sigma_{90}]$  was computed for different  $\varphi$  values. The proposed measurement is more sensible for maximum/minimum values of the gradient, and these correspond roughly to the position of the cross section dip. Thus the selected energy points were: 3050, 3060, 3083, 3090, and 3093 MeV.

In order to take into account the initial state radiation of the two colliding particles, the cross section at each energy point was obtained by a Monte-Carlo simulation of 100000 events. The rate at each energy point was then smeared with a Gaussian distribution centered in the simulated point with a width, sigma, equal to the rate error. The Gaussians at the selected energy points were then considered by the fitting routine. To define the precision of our parameters this procedure was iterated 100 times, and the expected precision was obtained by propagating the standard cross section errors. The rates at each energy point and hence our proposed measurements strictly depend on the collected integrated Luminosity per point. Assuming that one full day of data taking is dedicated to each energy point, a total of five days of beam time should be enough to perform our measurement. The expected integrated Luminosity was determined assuming an injection efficiency of 0.8, and a reconstruction efficiency for the selection of the different investigated channels: 0.67, 0.38, and 0.20 for  $p\bar{p}$ ,  $\rho\pi$ , and  $5\pi$  respectively.

Figure 6 shows the expected precision plotted as function of the integrated Luminosity for different assumptions of the relative phase for the  $p\bar{p}$  and the  $\rho\pi$  final states. As expected, the precision of the fit increases with the square root of the integrated Luminosity. The missing symmetry between the angular regions  $0^\circ$ - $90^\circ$  and  $90^\circ$ - $180^\circ$ , as shown in Figs. 3, 4, and 5, causes a lower sensitivity for larger relative phase values.

The precision of the relative phase measurement has shown a rather weak sensitivity on how the total integrated luminosity is shared between the different energy points. Figure 7 shows the relative phase precision as function of the  $L_2/L_1$  ratio, where  $L_1$  and  $L_2$  are the integrated Luminosities according to the  $L_1:L_1:L_2:L_2:L_1$  “configuration” of our five points set. The peculiar integrated Luminosity ratio 1:1:0.5:0.5:2 is also reported. We have hence selected the more conservative option for the luminosity ratio: 1:1:1:1:1, the same integrated Luminosity for each energy point. Assuming a Luminosity of  $2 \cdot 10^{32} \text{ cm}^{-2}\text{s}^{-1}$ , a total integrated Luminosity of  $14 \text{ pb}^{-1}$  has been requested for each selected energy value.

One more energy point is needed to have a stable fitting procedure with three free parameters:  $\Delta\varphi$ , the relative phase,  $\sigma_{cont}$ , the cross section at the continuum, and  $B_{out}$ , the branching ratio of the final state. At the  $J/\psi$  peak a large integrated Luminosity has already been collected during

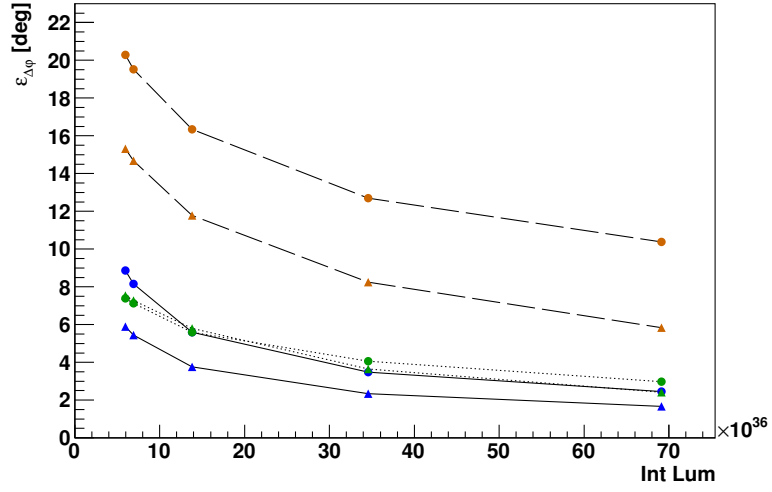


**Figure 6:** Expected precision ( $\epsilon_{\Delta\phi}$ ) plotted as function of the integrated Luminosity ( $[cm^{-2}]$ ) for the  $p\bar{p}$  (circles) and  $\rho\pi$  (triangles) final states and for different relative phases:  $10^\circ$  (dotted line),  $90^\circ$  (full line), and  $170^\circ$  (dashed line).

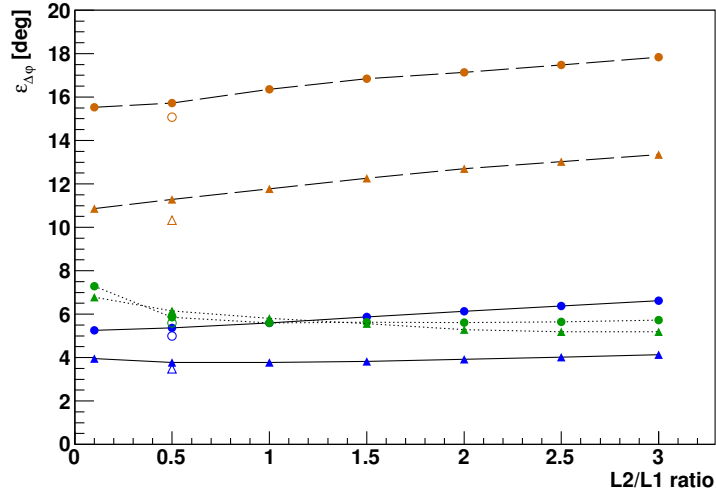


**Figure 7:** Expected precision ( $\epsilon_{\Delta\phi}$ ) plotted as function of the  $L_2/L_1$  ratio for the  $p\bar{p}$  (circles) and  $\rho\pi$  (triangles) final states and for different relative phases:  $10^\circ$  (dotted line),  $90^\circ$  (full line), and  $170^\circ$  (dashed line). The precision expected with the integrated Luminosity ratio 1:1:0.5:0.5:2 is reported here with open circles and open triangles.

previous data taking runs: this point is thus added to the above described five points set.

According to [8] we estimated the systematic errors, that have been rescaled according to the lower considered cross sections. They are not sizeable, and, in order to be more conservative, rather than considering the usual uncertainty evaluation procedure, we directly added them to the

estimated statistical uncertainties.

In the  $p\bar{p}$  final state case, the data in the literature suggest a relative phase around  $90^\circ$ : the overall obtained uncertainties for the three free parameters are quoted in Table 1. The statistical significance is good enough to discriminate between different theoretical predictions.

$\Delta\varphi$ [ $^\circ$ ]	$\Delta\sigma$ [pb]	$\Delta B_{out}/B_{out}$
6.1	0.9	$2 \cdot 10^{-3}$

**Table 1:** Expected precisions at  $\Delta\varphi = 90^\circ$  for a three parameters fit; systematic uncertainties have been accounted for.

At the selected beam energies, the required integrated Luminosities were collected by BESIII during the 2012 data taking run. An energy point close to 3083 MeV was already collected for other studies, and has then been included in the considered data set. Data selection procedures and data quality checks have already performed, and the physics analysis is ongoing. During the same 2012 BESIII data taking run, more energy points, albeit with a lower integrated Luminosity, were collected for a  $J/\psi$  resonance scan. These points will be included in the analyzed data set for the described measurement and could increase the precision in the determination of the free parameters.

This work was supported in part by Università degli Studi di Torino, Regione Piemonte, INFN Sez. Torino, and IHEP Beijing.

## References

- [1] A.M. Boyarski et al., Phys. Rev. Lett. 34, 1357 (1975).
- [2] J.Z. Bai et al., Phys. Lett. D 355, 374-380 (1995).
- [3] R. Baldini, C. Bini, E. Luppi, Phys. Lett. B404, 362 (1997).
- [4] R. Baldini et al., Phys. Lett. B444, 111 (1998).
- [5] L. Kopke and N. Wermes, Phys. Rep. 174, 67 (1989).
- [6] J. Jousset et al., Phys. Rev. D41,1389 (1990).
- [7] M. Suzuki et al., Phys. Rev. D60, 051501 (1999).
- [8] M. Ablikim et al., Phys. Rev. D 86, 032014 (2012).
- [9] D.M. Asner et al., Physics at BES-III, arXiv:0809.1869v1 [hep-ex] (2008)